Diffraction Regimes and Talbot Effect

MD Shafiul Alam

Laboratory Practice II

March 2019

Department of Physics and Mathematics
University of Eastern Finland

Md Shafiul Alam *Diffraction Regimes and Talbot Effect*, 19 pages
University of Eastern Finland
Master's Degree Programme in Photonics

Supervisors Henri Pesonen

Abstract

In this work, Talbot effect was studied by an experimental setup of light source and camera. The aim is to obtain self-images of a grating at different Talbot distances and to compare it with the simulated diffraction pattern obtained for these distances. For this purpose, high intensity Talbot effect was recorded at various distances along the optical rail with a CMOS camera and these distances were used to obtain intensity pattern for integer and fractional Talbot length. Experimentally obtained intensity pattern were compared with simulated pattern and quite similar intensity pattern was observed for integer and fractional Talbot length with some variations in experimentally obtained intensity patterns.

Keywords: self images; Talbot; intensity

Contents

1 Introduction **1**

2 Theory **3**

2.1 Diffraction of Light 3

2.2 Diffraction Grating 4

2.3 Angular Spectrum Representation Of Propagated Field 5

2.4 Talbot Effect 6

3 Experiment and Measurements **8**

4 Results and Discussions **10**

5 Conclusions **15**

References **16**

Appendix **18**

A Matlab Code 18

Chapter I

Introduction

Diffraction is one of the most important inherited properties of wave which refers to the bending of wave when travelling through an aperture or a slit. The underlying reason for this physical phenomenon is the interference of light which can be described by Huygens Fresnel principle. The condition for the diffraction to be occur is that wavelength of the wave must be comparable to the size of the slit [1]. In optics diffraction gratings are used to observe diffraction phenomena like dispersion of light and it is consisting of closely packed grooves that are cut out with a regular spacing between them. Diffraction gratings can be constructed as either transmissive or reflective way [2]. Basically, there are two types of diffraction phenomena can be observed: Fresnel (near field approximation) and Fraunhofer diffraction (far field approximation). Due to its many practical importance diffraction is used for various fields of science and technology such as optical holography, X-Ray diffraction, optical spectroscopy etc. Talbot effect, also known as self-imaging or lens less imaging was first discovered by Henry Fox Talbot in 1836. The effect is observed when a plane wave incident on a periodic structure i.e. diffraction grating, self-images of the grating is produced at certain distances behind the grating [3]. Talbott effect has a range of practical implication such as image processing, electron microscopy, plasmonic, X-Ray and Bose-Einstein condensation [4]. In this work, Talbot effect was studied experimentally by a laboratory setup that contain laser source, diffraction grating and a CMOS camera as a detector. Experimentally obtained integer and fractional Talbot length were used to compare with simulated data. The simulation was based on electromagnetic field propagation which will be discussed on the 2nd chapter. Also, the theoretical background of diffraction and Talbot effect will also

be discussed in this chapter. The experimental procedure will be briefly discussed in the 3rd chapter while the findings of experiment as well as simulation will be explained in the 4th chapter. Finally, the whole work will be summarized in the conclusion part. The MATLAB Code is attached at the end of the report.

Chapter II

Theory

In this chapter fundamental theory of light diffraction as well as diffraction grating will be described. Also, the basic theory of electromagnetic field propagation on which MATLAB simulation is based on, will also be described.

2.1 Diffraction of Light

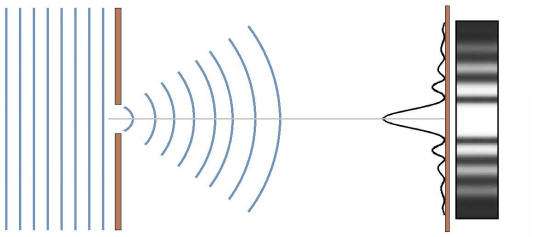

Figure 2.1: Effects of diffraction phenomena and the formation of dark and bright fringes

When a light wave passes through an obstacle or an aperture, a portion or part of the wavefront is changed in amplitude and phase. After passing the obstacle various segments of the wavefront interfere and therefore a diffraction patterns appears in the screen. So, diffraction is a kind of interference. The only distinction is that in diffraction, large number of waves superposed with each other.

According to the Huygens principle each point of an advancing wavefront act as the source of a secondary wavelets and the shape of the wavefront acts like the

envelope of the secondary wavelet. But this principle has some limitations as it also means the spreading of wave even behind the source which does not happen in some case e.g. laser. This limitation of phase and amplitude was overcome by Fresnel as he recognized the necessity of angular dependency of secondary wave. In the Huygens principle he added that the amplitude of the optical field at any point beyond the aperture is the superposition of secondary wavefront. After passing the aperture the secondary wavefronts interfere with each other, depending on the optical path length and phase, there can be constructive or destructive interference and consecutive dark and bright fringes appear in the screen depending on the interference pattern [5]. A typical diffraction phenomenon is shown in the Figure 2.1. Based on the distance from the aperture and screen diffraction can be two types: Fresnel or near field diffraction and Fraunhofer or far field diffraction.

If we consider the aperture that is illuminated by a plane wave and the plane of observation are very close to each other, we find the image of the aperture with some fringing around it, in the screen of plane of observation. The further movement of the image plane results in the more structured image with more visible fringes. This type diffraction is called Fresnel or near field diffraction. If the distance between the observation plane is increased considerably the image pattern of the aperture changes significantly in size although the movement has not any effect in the shape. This type of diffraction is known as Fraunhofer or far field diffraction. However, enough reduction of wavelength can turn the Fraunhofer case to Fresnel case and further reduction can cause the disappearance of fringe in the image plane. [5].

2.2 Diffraction Grating

A diffraction grating is a set of diffracting elements which can be either transmitting or reflecting elements separated by a specific distance. The distance must be comparable to the wavelength of the light used in the process. The basic property of a diffraction grating is the spatial modulation of refractive index. A series of transparent slits are used as transmitting elements in an opaque screen while reflecting grooves on a substrate are used as reflecting elements. The first diffraction grating was a half inch wide grating with fifty-three apertures which was developed by American astronomer, David Rittenhouse [7], in 1785. Diffraction grating can be different types: reflection grating, transmission grating, master grating and replica

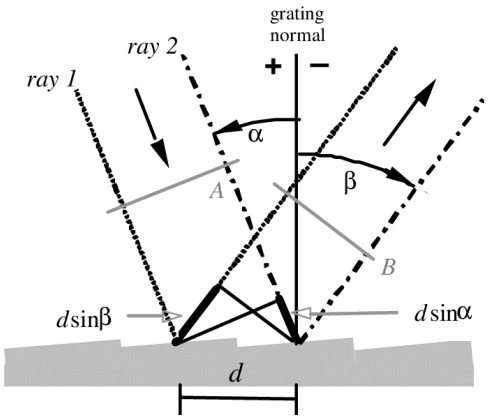

Figure 2.2: Two plane wave are incident on the diffraction grating with groove spacing d. Both incident waves are in phase at the plane A and according to the condition of constructive interference, they are also in phase after diffraction at plane B. [6]

grating. Reflection grating formed on reflective surfaces while the transmission grating formed on transmission surfaces. Master grating is based on surface relief pattern which is created by holographic recording while the surface relief pattern of replica grating is formed by molding the relief pattern of another grating. In a diffraction grating with a groove spacing d constructive interference occurs when the light diffracted from each grating groove is in phase with the light diffracted from any other groove. Figure 2.2 illustrates the diffraction incident for the planer wave front. From the condition of diffraction, it is known that constructive interference occurs when the path difference equals to the integral multiple of wavelength λ.The path difference between consecutive groove is $d\sin\alpha + d\sin\beta$. The relationship that gives the constructive interference condition is given by

$$m\lambda = d\sin\alpha + d\sin\beta \tag{2.1}$$

Here, m is the diffraction order. For, $\mid m\lambda/2 \mid < 2$ propagating diffraction order is obtained. [8]

2.3 Angular Spectrum Representation Of Propagated Field

If we consider a uniform plane wave with $E_0(x) = 1$ incident on a grating, the periodic transmission function $t(x)$ has value 1 only in the slit region while it is zero

in other areas and can be represented as

$$t(x) = \begin{cases} 1, & \text{when } 0 \leq x \leq fd. \\ 0, & fd \leq x \leq d. \end{cases} \tag{2.2}$$

Here, f is the fill factor($f = 0.1$) of the grating and d is the grating period ($d = 150\mu m$). The transmitted field can be expressed as

$$E_t(x, z = 0) = \sum_{m=-M}^{M} t_m \exp(ik_{xm}x) \tag{2.3}$$

The summation is taken from $-M$ to $-M$ for the numerical representation of the field where M is finite but sufficiently large integer number. The Fourier coefficients are given by

$$t_m = \frac{1}{d} \int_0^d t(x) E_0(x) \exp(-ik_{xm}x) dx \tag{2.4}$$

For the field transmitted through the grating, the angular spectrum is expressed in a discrete form

$$E_t(x, z) = \sum_{m=-M}^{M} t_m \exp(ik_{xm}x + ik_{zm}z) \tag{2.5}$$

Here,

$$t(x) = \begin{cases} (k^2 - k_{xm}^2)^{\frac{1}{2}} & \text{if } k_{xm}^2 \leq k^2 \\ i(k_{xm}^2 - k^2)^{\frac{1}{2}}, & \text{if } k_{xm}^2 > k^2. \end{cases} \tag{2.6}$$

is the z component of the wave vector where $k = 2\pi/\lambda$, the number of propagating orders can be calculated using the relation of $\sin\theta_m = m\lambda/d$. But if $sin\theta_m > 1$, the diffraction angle becomes complex and the diffraction orders are evanescent.

2.4 Talbot Effect

H. F. Talbot [9] first observed when a plane wave is incident on a diffraction grating, different optical patterns are observed at different planes with z = constant from the grating. This appearance of perfectly distinct and well-defined band after the diffraction of plane wave is known as Talbott effect. It is found that the field reproduce itself or its image appears at different position of z which are the integral

multiples of the Talbot distance. Lord Rayleigh, [10] in 1881 proved that this effect is due to the diffraction interference of highly spatially coherent plane wave.

If we consider a plane wave with wavelength λ incident on a diffraction grating with transmittance $t(x)$ and grating period d, after diffraction an exact image of the grating will be appeared in a series of equally spaced plane known as Talbot planes. The Talbot effect satisfy the following relation.

$$L_s = s\frac{2d^2}{\lambda} \tag{2.7}$$

Here, s is the integer number which is also known as self-imaging number and for $s = 1$, we get Talbot distance $L_T = 2d^2/\lambda$. Cowley and Moodie [11–14] suggested that the factor 2 can be removed by considering s in an odd integer which means half a period lateral shift of the object image with respect to the object. So, it appears, for $m = 1$, $L_T = 2d^2/\lambda$ is the secondary Talbot length and $2L_T$ is the primary Talbot length. On the other hand, fractional Talbot images are formed in the fractional multiple of L_T i.e. $L = m/n(d^2/\lambda)$. Here, m and n are coprime integers [4, 15]. Sub-images appear at the fractional Talbot length and they contain smaller lateral period with respect to the self images. Sub-images are constructed at the sub Talbot plane when the higher diffraction order interfere destructively with lower diffraction orders. Sub images contains smaller fraction of the oroginal lateral periodicity [16].

Chapter III

Experiment and Measurements

In this chapter, laboratory setup and experimental procedure for observing Talbot effect will be discussed.

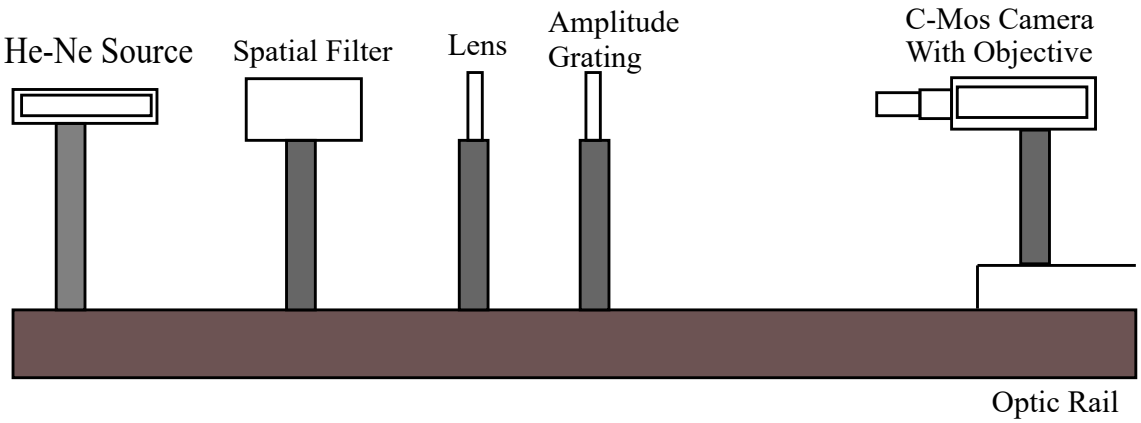

Figure 3.1: Laboratory setup for observing Talbot Effect

The experimental setup for the Talbot effect is illustrated in the Figure 3.1. During the measurement a diffraction grating of $d = 150\ \mu m$ and fill factor $f = 0.1$ was illuminated by a Helium-Neon laser of wavelength $\lambda = 633\ nm$. For capturing the self-image of the grating, a CMOS camera of resolution 1280x1024 pixels and the pixel size of 5.2 μm was used. The distance between the grating and the detector was changed by moving the CMOS camera on a trail to get the Talbot images and fractional Talbot images of the grating. Coherent light wave from the He-Ne laser source passes through a spatial filter and collimating lens before incident on the grating. The spatial filter was used to remove the unwanted multiple peaks

in diffraction pattern and pass central maxima while collimating lenses are used to control the field of view, collection efficiency and spatial resolution of the setup [2,17]. The images of the diffraction pattern captured by the microscopic objective were ten times magnified. The whole setup was mounted on an optical table which is very much sensitive to vibration. This experiment was performed on a dark room to get rid of stray light.

Chapter IV

Results and Discussions

In this section of the report, experimental results of the Talbot effect will be presented and will be compared with the simulated intensity pattern of Talbot distances and fractional Talbot distances. Also, self-images of the diffraction grating for integer and fractional Talbot distances will also be presented. In the first part of the experiment, Talbot images of the diffraction grating were captured by the CMOS camera by changing the position of the camera along the optic trail. It is found that at certain distances behind the grating, the diffraction grating replicate itself and high intensity Talbot images were recorded at these distances. The distance between these identical Talbot images were found to be 37mm and their distance from the diffraction grating are integer multiple of Talbot length. However, the rescaled patterns are found in fractional Talbot length. The integer Talbot length images were observed in 323mm, 360mm and 397 mm and they are presented in figure 4.1.

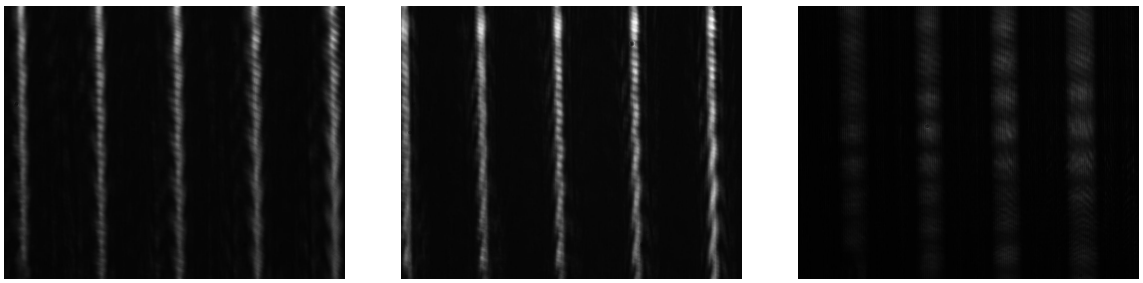

(a) (b) (c)

Figure 4.1: Experimentally observed integer Talbot length images at (a) 323 mm, (b) 360mm and (c) 397mm

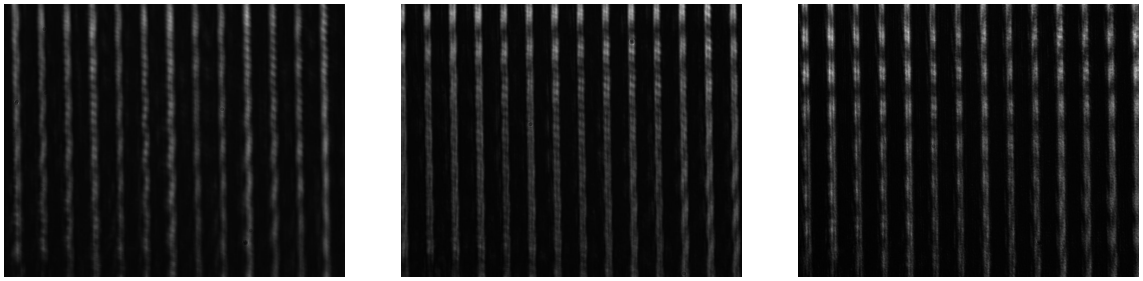

(a) (b) (c)

Figure 4.2: Experimentally observed integer Talbot length images at (a) 349 mm, (b) 373 mm and (c) 385 mm

Also, fractional Talbot length images were observed in 349 mm, 373 mm and 385 mm which are presented in figure 4.2. The Talbot length L_T was calculated using

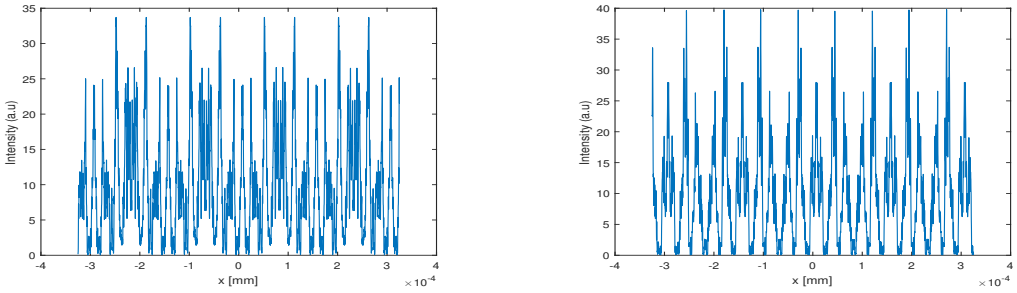

(a) (b)

Figure 4.3: Intensity pattern obtained from (a) simulation and (b) experiment at $9L_T$

Eq.(2.7) and found to be 35.54 mm. Using this value, integer and fractional Talbot lengths were calculated. The integer multiple of Talbot length were calculated at $9L_T$ (319.8mm), $10L_T$ (355.54mm) and $11L_T$ (390.94mm) and high intensity is observed in these regions. For getting the intensity pattern, MATLAB simulation code was used which is based on Eqs. (2.2) – (2.6). While simulation, the magnification factor of the camera was considered.Also, experimental counterparts of the

simulated intensity patterns were plotted which are based on the same code. Fig. 4.3, Fig. 4.4 and Fig. 4.5 exhibits the intensity pattern of integer multiple of Talbot length for simulated and measured Talbot images.

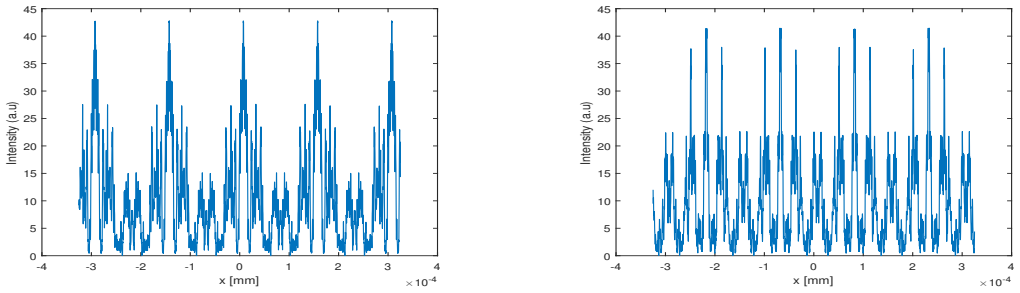

(a) (b)

Figure 4.4: Intensity pattern obtained from (a) simulation and (b) experiment at $10L_T$

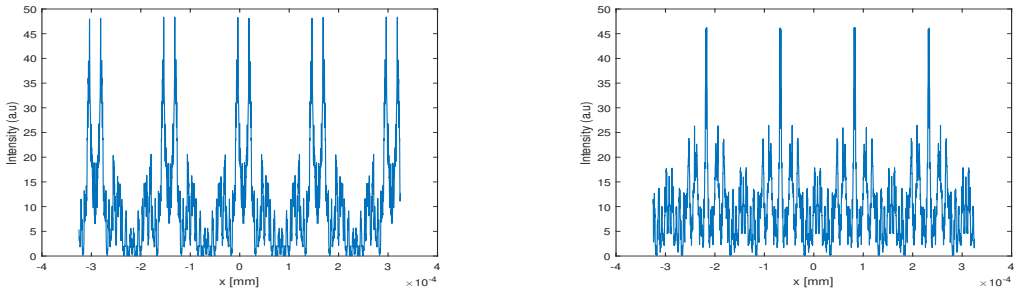

(a) (b)

Figure 4.5: Intensity pattern obtained from (a) simulation and (b) experiment at $11L_T$

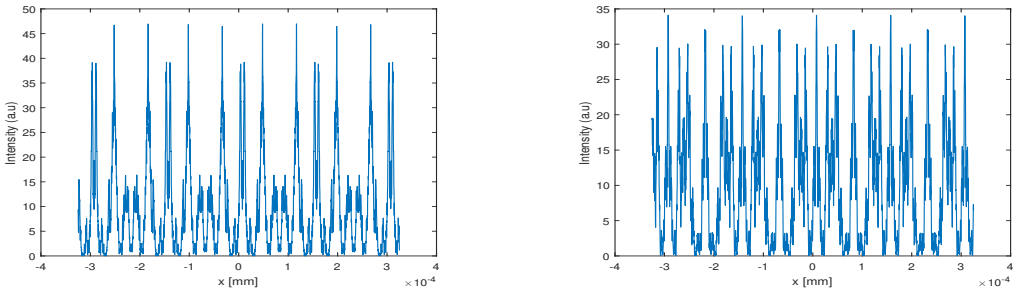

(a) (b)

Figure 4.6: Intensity pattern obtained from (a) simulation and (b) experiment at $\frac{49}{5}L_T$

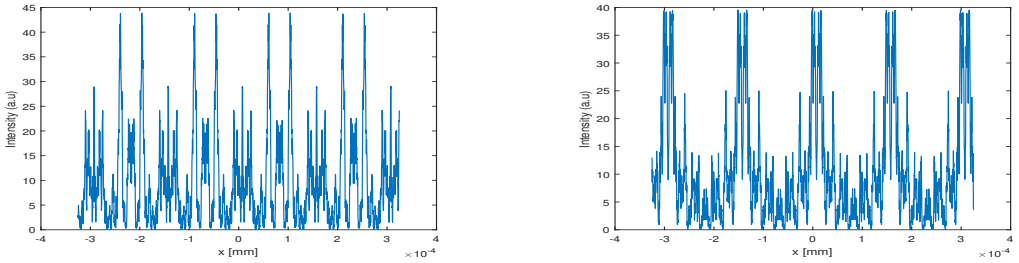

(a) (b)

Figure 4.7: Intensity pattern obtained from (a) simulation and (b) experiment at $\frac{53}{5}L_T$

More sharp and high intensity peaks are observed in simulated pattern.The difference is clearly visible in Fig. 4.4 and Fig. 4.5 where it is found that some extra peaks are appeared in experimental intensity pattern while in simulated intensity pattern these extra peaks are suppressed. The reason for these errors in experimental data is may be because of stray light which could be avoided by taking the image of the background. Also, the focusing of the CMOS camera may not be perfect which also contribute in the experimental error and the effect is particularly visible in the Fig. 4.1(c) and therefore appearance of extra peaks around the high intensity peaks in Figure 4.5(b). On the other hand, the collimation of light beam by collimating lens may not be perfect while in simulation it was assumed that light beam that pass through the collimating lens are fully collimated. Also, the spatial filter may not work perfectly which allows the multiple order energy peaks to pass through the

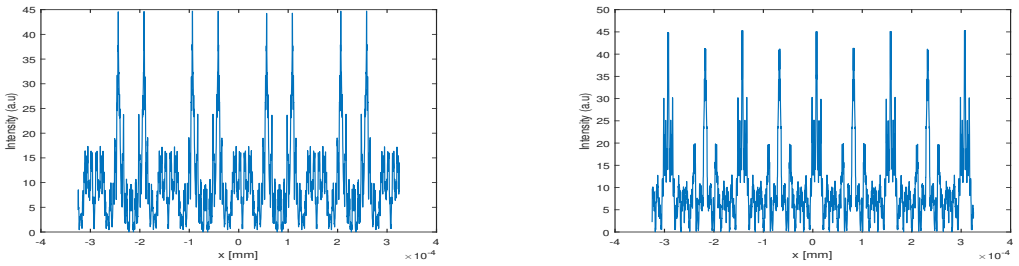

(a) (b)

Figure 4.8: Intensity pattern obtained from (a) simulation and (b) experiment at $\frac{54}{5}L_T$

filter. Fractional multiple of Talbot length were calculated at $\frac{49}{5}L_T$ (348.29 mm), $\frac{53}{5}L_T$ (376.72 mm), $\frac{54}{5}L_T$(383.83 mm). Fig. 4.6, Fig. 4.7 and Fig. 4.8 exhibit the intensity pattern of fractional Talbot lengths for simulated and measured Talbot images. The difference between simulated and experimentally obtained intensity pattern is much less now, may be due to more focused camera although extra peaks are still visible in experimentally obtained intensity pattern. However, it is observed that with increasing fractional Talbot length the intensity decreases which is due to divergence of fields with increasing distances.

Chapter V

Conclusions

In this experiment, Talbot effect and diffraction phenomena were studied. The Talbot effect was observed experimentally, and self-image of the diffraction grating was recorded at different integer and fractional Talbot distances. A He-Ne laser source, diffraction grating with $d = 150\mu m$ and fill factor $f = 0.1$, and a CMOS camera as a detector were used for studying Talbot effect. Simulation was performed to compare the theoretical integer and fractional Talbot length with their experimental counterparts. The simulation was based on electromagnetic field propagation and in total 237 diffraction orders were taken with 5000 sampling points. Self iamges and subimages are obtained at integer and fractional multiple of Talbot length ($35.54mm$). The intensity plot for the integer and fractional multiple of Talbot length were found to be quite similar in experimental and simulation case although some errors were associated with them. With enough precautions these errors could be avoided.

References

[1] T. S. Rappaport, *Wireless communications: Principles and practice*, 2nd ed. (Prentice Hall, 2002).

[2] Edmund Optics, https://www.edmundoptics.com/ (visited on 2019-18-03).

[3] A. Wang, P. Gill, and A. Molnar, "Light field image sensors based on the Talbot effect," *App. Opt.* **48(31)**, 5897–5905 (2009).

[4] J. Wen, Y. Zhang, and M. Xiao, "The Talbot effect: recent advances in classical optics, nonlinear optics, and quantum optics," *Adv. Opt. Photon.* **5(1)**, 83–130 (2013).

[5] E. Hecht, *Optics*, 5th ed. (Pearson Education, 2017).

[6] The star Garden, http://www.thestargarden.co.uk (visited on 2019-18-03).

[7] D. Rittenhouse, "Explanation of an optical deception," *Trans. Amer. Phil. Soc* **2**, 37–42 (1786).

[8] C. Palmer, *Diffraction Grating Handbook*, 6th ed. (Newport Corporation, 2005).

[9] F. Talbot, "Facts relating to optical science. No. IV," *Philos. Mag.* **9**, 401–407 (1836).

[10] L. Rayleigh, "On copying diffraction gratings and some phenomena connected therewith," *Philos. Mag* **11**, 196–205 (1881).

[11] J. M. Cowley and A. F. Moodie, "Fourier images I. The point source," *Proc. Phys. Soc.* **70**, 486–496 (1957).

[12] J. M. Cowley and A. F. Moodie, "Fourier images II. The out-of-focus patterns," *Proc. Phys. Soc.* **70**, 497–504 (1957).

[13] J. M. Cowley and A. F. Moodie, "Fourier images III. Finite sources," *Proc. Phys. Soc.* **70**, 505–513 (1957).

[14] J. M. Cowley and A. F. Moodie, "Fourier images IV. The phase grating," *Proc. Phys. Soc.* **70**, 378–384 (1957).

[15] G. S. Spagnol and D. Ambrosini, "Talbot effect application: measurement of distance with a Fourier-transform method," *Meas. Sci. Technol* **11**, 77–82 (1999).

[16] C. M. C. R. M.-S. Kim, T. Scharf and H. P. Herzig, "Talbot images of wavelength-scale amplitude gratings„" *Opt. Express* **20** (2012).

[17] Ocean Optics, https://oceanoptics.com/ (visited on 2019-18-03).

Appendix A

Matlab Code

```
function [It,x]=talbot_mm(z);
%
% Field behind binary amplitude grating at distance z
%
% z = propagation distance
% d = period of the grating
% f = fill factor
% Dx = size of the calculation window
% N = number of the sampling points
% M = number of included diffraction orders
% lambda = wavelength

lambda=633e-9;
N=5000;
M=237;
Dx=0.65e-3; % calculated by given parameter
f=0.1;
d=150*10^-6;
% z = [0.0494,0.0247,0.0165,0.01234,0.0082,0.0049]
k=2*pi/lambda;
x=linspace (-Dx/2, Dx/2, N);
Et=zeros (size(x));

for m=-M:M;
% Add here the expressions for the complex amplitude coefficients
% tm and t0 that can be analytically solved from Eq. (2.4.3)
tm=i/(2*pi*m) *(exp(-i*2*pi*m*f)-1)
if m==0
```

```
tm=f;
end
kxm=2*pi*m/d;
kzm = sqrt(k^2- kxm.^2);
Et=Et+tm*exp(i*(kxm*x+kzm*z));
It=abs (Et).^2;
end
figure;
plot((x), It*10^2)
x label ('x [mm]')
y label ('Intensity (a.u)')
```